ELSEVIER

Journal of Crystal Growth 226 (2001) 223–230

JOURNAL OF CRYSTAL GROWTH

www.elsevier.nl/locate/jcrysgro

# Epitaxial Fe/MgO heterostructures on GaAs(0 0 1)

C. Martínez Boubeta[a,*], E. Navarro[a,b], A. Cebollada[a], F. Briones[a], F. Peiró[c], A. Cornet[c]

[a] *Instituto de Microelectrónica de Madrid-IMM (CNM-CSIC), Isaac Newton 8 (PTM) Tres Cantos, E-28760 Madrid, Spain*
[b] *Departimento Física Aplicada, Facultad de Veterinaria, Universidad Complutense, E-28040 Madrid, Spain*
[c] *Electronic Materials and Engineering, Facultat de Fisica, Universitat de Barcelona, Av. Diagonal 645-647, E-08028 Barcelona, Spain*

Received 25 March 2001; accepted 3 April 2001
Communicated by M. Schieber

**Abstract**

Epitaxy of high quality Fe/MgO heterostructures on GaAs(0 0 1) substrates has been achieved by combined use of sputtering and laser ablation deposition techniques. Growths of Fe thin structures on MgO buffered GaAs is studied for a wide range of deposition temperatures. The Fe crystalline quality continuously increase with deposition temperature although a transition from 2D continuous films towards discontinuous 3D-like Fe structures is found between 300°C and 400°C. Insulator on metal epitaxy is also confirmed as MgO layers are found to epitaxially grow on previously deposited Fe/MgO/GaAs thin films. From these results, it is shown that Fe/MgO superlattices can be fabricated on semiconductor substrates by appropriate selection of growth conditions. © 2001 Elsevier Science B.V. All rights reserved.

*PACS:* 81.15.Cd ; 81.15.Fg ; 75.70. − i

*Keywords:* A1. Interfaces; A3. Superlattices; B1. Metals; B1. Oxides; B2. Magnetic materials

## 1. Introduction

The fabrication of new metal/insulator ferromagnetic heterostructures has attracted a lot of attention in recent years, both for the interest of the fundamental properties that these systems exhibit, as well as for the potential technological applications, specially in the field of magnetoelectronics [1]. This range of applications cover for example the fabrication of high sensitivity magnetic field sensors, hard disk read heads [2] and specially magnetic random access memories (MRAM) [1]. For many of these devices, the fundamental property exploited is the so-called tunnel magnetoresistance (TMR), in which the tunnel resistivity of the device depends on the relative magnetic configuration of its two magnetic electrodes [3]. On the other hand, a relevant advance would be the fabrication of this kind of devices on semiconductor heterostructures, with the aim to integrate semiconductor and magnetic systems as a final goal for a next generation of magnetoelectronic systems. Within

*Corresponding author. Tel.: +91-806-0700; fax: +91-806-0701.
*E-mail address:* boubeta@imm.cnm.csic.es (C. Martínez Boubeta).

0022-0248/01/$ - see front matter © 2001 Elsevier Science B.V. All rights reserved.
PII: S0022-0248(01)01397-5

WD EX1084
Western Digital v IP Bridge
Page 223

this framework, a key aspect in the fundamental understanding of the physical properties of these structures is their single crystalline character, also termed epitaxial in case of thin films. Many efforts have been devoted in this line to obtain epitaxial magnetic thin films, specially Fe, on III–V semiconductor substrates, such as GaAs [4], or also II–VI compounds like ZnSe. A common feature of all these structures is that the ferromagnetic layer is deposited directly onto the semiconductor surface, being therefore exposed to intermixing if deposited or annealed above relatively moderate temperatures.

Up to date, there are very few papers dealing with the epitaxy of metal/insulator superlattices, to mention for example the work by Kado on Ag/NiO [5] or TiAg/MgO [6] structures. Nevertheless, several results are already known on the MgO/GaAs(0 0 1) epitaxy [7–10], being demonstrated that MgO can be an excellent diffusion barrier for high temperature epitaxial growth on GaAs. On the other hand, the Fe/MgO(0 0 1) is nowadays a very well established system (see for example Ref. [11]), but very few works have reported either on the epitaxy of MgO on Fe(0 0 1) [12,13] or of Fe/MgO/Fe trilayered structures [14–16].

The aim of the present work is to present results on the study of the epitaxy of metal/insulator Fe/MgO heterostructures on MgO buffered GaAs(0 0 1) semiconductor substrates which, for the motivation described above, can be of great relevance in the field of ferromagnetic-semiconductor integrated magnetoelectronic systems. Following, and after a brief description of the experimental aspects, a detailed study on the growth temperature dependence of the Fe thin films morphology will be first presented. As a second part, results on the fabrication of two Fe/MgO epitaxial multilayered structures using different deposition temperatures will be shown and discussed.

## 2. Experimental procedure

GaAs(0 0 1) substrates were previously prepared in a separate molecular beam epitaxy (MBE) system where a 2000 Å GaAs epitaxial layer was grown to planarize the surface. Following, an amorphous $As_2$ layer was deposited at room temperature to avoid surface oxidation during transfer in air. Substrates were then loaded in a separate growth chamber with $2\times10^{-9}$ mbar base pressure and combined triode sputtering and laser ablation facilities, where the $As_2$ capping layer was desorbed by annealing at 450–500°C for 1 h. Total elimination of $As_2$ capping layer was checked by the appearance of the characteristic $(2\times4)$ GaAs(0 0 1) reflection high energy electron diffraction (RHEED) pattern. Subsequently, a 80 Å MgO buffer layer was grown at 450°C by normal incidence pulsed laser deposition from a monocrystalline MgO target in the pressure regime of $7\times10^{-9}$ mbar. An ArF excimer laser with $\lambda = 193$ nm and pulse of 17 ns working at 10 Hz repetition rate, and fluence slightly above the ablation threshold to avoid particle ejection, was used. Laser beam was focussed with an oscillating lens ($f = 200$ mm) on the rotatory target 40 mm away from substrate. Under this experimental conditions typical deposition rate is 0.17 Å/s. The role of this MgO buffer layer is twofold: it first serves as interdiffusion barrier to avoid incorporation of As from the substrate into the sample layers, and secondly, offers an appropriate symmetry and lattice match for the epitaxy of bcc Fe(0 0 1) layers. Onto this MgO buffer layer, Fe films were deposited by normal incidence triode sputtering in the same deposition system at $4\times10^{-4}$ mbar Ar pressure to optimize film quality [17] obtaining deposition rates between 0.1 and 0.2 Å/s, similar to those normally used in MBE. In all the structures fabricated, and to prevent films from oxidation, a 25 Å thick Pt capping layer was deposited by sputtering at room temperature in similar Ar conditions as the previously described Fe layer. The structure was checked insitu by RHEED and exsitu by X-ray diffraction (XRD) using Cu $K_\alpha$ radiation ($\lambda = 1.5418$ Å), Bragg–Brentano configuration, a secondary Cu monochromator and 1/4° slits. Surface micrographs were taken by atomic force microscopy (AFM). Some specific structures were also studied by transmission electron microscopy (TEM).

WD EX1084
Western Digital v IP Bridge
Page 224

## 3. Epitaxy of Fe single layers on MgO/GaAs(0 0 1)

We have previously shown the epitaxy of Fe/MgO/GaAs heterostructures [18] at a specific growth temperature. Here, a study covering a wide growth temperature range for deposition of the Fe film is presented. Different Fe structures were deposited on MgO buffered GaAs substrates at temperatures from room temperature (RT) up to 700°C. Results of the in situ structural characterization are shown in Fig. 1, were RHEED patterns for the clean GaAs substrate, MgO buffer, and the Fe films grown at several temperatures are presented for two different azimuths. In Fig. 1(a) and (b) we show the RHEED pattern of a clean GaAs(0 0 1) surface after As desorption and the MgO buffer layer, respectively. This serves as confirmation for the MgO(0 0 1)[1 0 0]‖GaAs (0 0 1)[1 0 0] epitaxial relation [19]. Growth of the iron layer on MgO is epitaxial for all temperatures studied, as shown in Figs. 1(c)–(e). In this case, the well known Fe(0 0 1)[1 1 0]‖MgO(0 0 1)[1 0 0] relation is observed. Worth to mention is the faceted nature of the Fe surface for RT deposition (Fig. 1(c)). This faceted morphology can be detrimental for the fabrication of magnetic tunnel junctions, where very flat surfaces are required, and is found to be suppressed after annealing at 400°C during 15 min (Fig. 1(d)). For Fe films grown at temperatures above 300°C, RHEED patterns are identical to the one shown in Fig. 1(e), and are characteristic for single crystalline flat Fe(0 0 1) surfaces. Pt RHEED patterns (not shown) are also indicative of its epitaxial nature, with Pt(0 0 1)[1 0 0]‖Fe(0 0 1)[1 1 0] registry. In this case, diffraction lines are broader due to the low temperature growth of the capping layer.

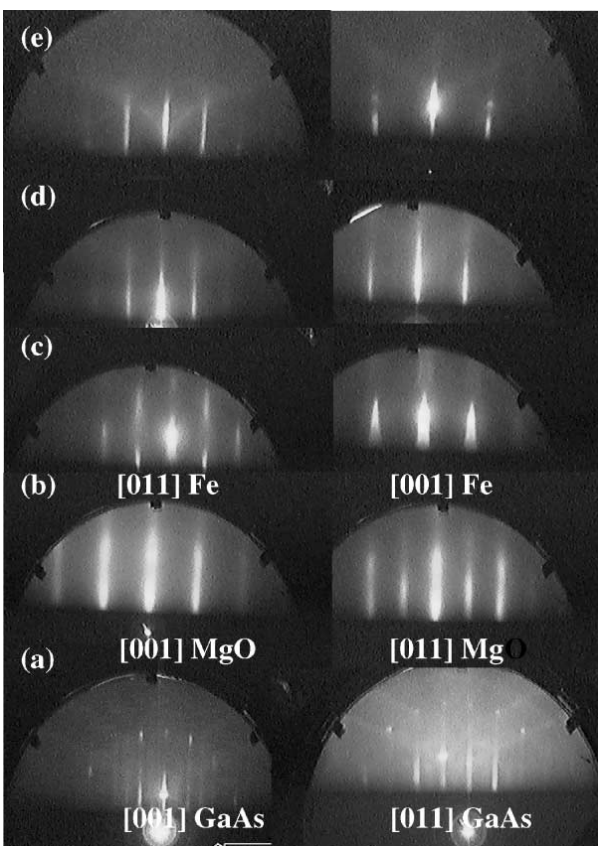


Fig. 1. RHEED patterns along [0 0 1] and [0 1 1] GaAs substrate azimuths for Fe/MgO/GaAs(0 0 1) structures with different Fe growth conditions. (a) GaAs, (b) MgO buffer layer, (c) Fe grown at RT, (d) Fe grown at RT and annealed at 400°C for 15 min, (e) Fe grown at 500°C.

An ex situ characterization of the crystalline structure for all grown samples was performed by XRD. In Fig. 2(a) we present the high angle XRD symmetric scan for a representative Fe film grown at 300°C. Peaks corresponding to Pt, MgO and Fe(2 0 0) reflections are clearly observed, together with the substrate GaAs(4 0 0) diffraction peak. It is remarkable the clear observation of both MgO buffer and Pt capping layer peaks despite of their small thickness (80 and 25 Å, respectively), which supports the crystalline character of both layers.

On the other hand, the Fe(0 0 1)[1 1 0]‖MgO(0 0 1)[1 0 0]‖GaAs(0 0 1)[1 0 0] epitaxial orientation concluded by RHEED characterization can be confirmed from XRD $\phi$-scans of Fe(1 1 0), MgO(2 2 0) and GaAs(2 2 0) asymmetric peaks, as shown in Fig. 2(b). The 45° in plane rotation of the Fe lattice with respect to the MgO film and GaAs substrate is clearly observed. Four characteristic peaks for the Pt(2 2 0) reflection are even detected, confirming the epitaxial nature of the capping layer.

Determination of both in- and out-plane interplanar distances as well as lattice distortion for the different Fe films was performed from analysis of data taken by combination of symmetric and

WD EX1084
Western Digital v IP Bridge
Page 225

asymmetric XRD scans yielding to the values shown in Table 1. $S_{\perp}$ and $S_{\parallel}$ correspond to the Fe lattice distortions along the directions perpendicular and parallel to the surface and are defined as $S_{\perp,\parallel} = (a_{\exp\perp,\parallel} - a_{\text{bulk}})/a_{\text{bulk}}$, where $a_{\exp\perp,\parallel}$ and $a_{\text{bulk}}$ are experimental and bulk Fe lattice parameters. The mosaic spread is the FWHM ($\omega$) of the rocking curve for the symmetric diffraction peak and Grain size is the crystalline coherence length along the growth direction estimated applying Scherrer's equation to the breadth of the symmetric reflections.

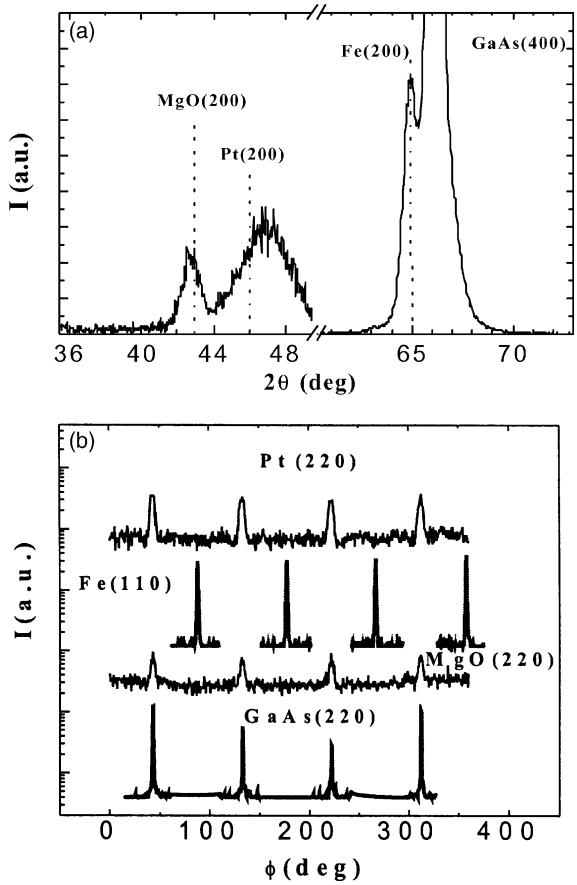


Fig. 2. (a) High Angle XRD pattern for a Pt/Fe/MgO/GaAs(0 0 1) structure with Fe grown at 300°C. Vertical lines indicate positions for bulk MgO, Pt and Fe(2 0 0) peaks (b) $\phi$-scans of asymmetric reflections for substrate and different layers. Curves are vertically offset for clarity.

As can be seen in Table 1, all lattice parameters are close to bulk values within less than 0.5%. There exists a small out of plane expansion (0.3–0.4%) for growth at low temperatures that evolves towards out of plane contraction (0.2–0.4%) for high growth temperatures. This behaviour is accompanied by a zero or moderate in plane expansion that increases up to 0.2–0.3% for high growth temperatures. This can be interpreted as a small Fe lattice accommodation due to the 3.8% lattice mismatch with respect to MgO upon 45° in plane rotation. Finally, mosaicity and grain size gradually decrease and increase, respectively, for higher growth temperatures, as a consequence of a higher crystalline quality.

At this point, the main conclusion from the structural point of view is that it is possible to obtain epitaxial Fe(0 0 1) thin films on MgO/GaAs surfaces with improved crystallinity at higher growth temperatures. Next is the detailed characterization of the surface morphology at the nanometric level for all the fabricated structures, for what AFM is the best-suited technique. Since all structures were measured ex situ, the information obtained will be that of the topmost layer, in this case the Pt capping. Samples grown at 200°C and below exhibited very flat, continuous and featureless surfaces in the lateral areas explored (typically 5–10 μm wide), with typical rms roughness around 3 Å. Mention that no significant difference could be observed between a film grown

Table 1
Structural parameters for selected Fe films obtained from XRD characterization

| Growth temperature (°C) | RT | 100 | 300 | 500 | 700 |
|---|---|---|---|---|---|
| $S_{\parallel}$ | 0% | 0% | 0.2% | 0.3% | 0.2% |
| $S_{\perp}$ | 0.3% | 0.4% | 0.1% | − 0.4% | − 0.2% |
| Mosaic | 1.5° | 1.1° | 1.1° | 0.9° | 0.9° |
| Grain size (Å) | 90 | 90 | 90 | 110 | 110 |

WD EX1084
Western Digital v IP Bridge
Page 226

at RT and another one grown at the same temperature and annealed at 400°C. This is an indication that the faceting observed by RHEED in the RT films amounts for a very small vertical roughness, that can even be hidden by the later deposition of Pt at RT. For growth temperatures of 300°C and above, film surfaces were characterized by the gradual appearance of morphological features that were growth temperature dependent. In Fig. 3, we show AFM scans for samples grown at 300°C, 400°C, 500°C and 700°C, in which the morphology evolution with growth temperature becomes evident. In Fig. 3(a), the surface morphology for a sample grown at 300°C exhibit characteristic pinholes uniformly distributed all over the scanned area with lateral dimension of these pinholes range from 280 up to 1600 Å. Morphology for a sample grown at 400°C is shown in Fig. 3(b), and exhibits a structure that has evolved from holes to a dendritic like structure, the previous uncovered substrate regions becoming elongated. Further increase of growth temperature to 500°C leads to the formation of isolated Fe platelets, obtained by the lack of coalescence of the Fe film at this growth temperature, increasing even more the uncovered area with respect to 400°C growth temperature (Fig. 3(c)). Finally, deposition at the highest temperature (700°), leads to the formation of well defined Fe islands, many of them of squared and rectangular shapes, and with the polygons sides parallel to the Fe[1 0 0] and [0 1 0] directions (Fig. 3(d)). From AFM profile measurements it is proved that island depths for Fe grown at 700°C, which is also the case where Fe islands are more separated from each other, are in agreement with nominal film thickness. On the other hand, for intermediate growth temperatures where islands are closer (600°C) or even lower temperatures (400–300°C) where elongated and pinhole uncovered regions are even narrower, depths measured with AFM gradually reach smaller values. This is probably due to the big size of the AFM tip compared with the lateral extent of the uncovered region being therefore not possible to reach the bottom area. This growth temperature dependent film morphology has also been observed in the Pt/MgO(1 1 0) system [20], and is a common behaviour obtained in different heteroepitaxial systems, being interpreted either using thermodynamic (difference in free surface energies of substrate and deposit) or kinetic arguments (energetic barriers for surface and step edge diffusion, modified via lattice distortion at the island edges) [21]. The interpretation for the narrow distribution of island sizes observed for 700°C growth temperature can be understood considering the strain dependence of the adatom diffusion barriers: after and island is formed, the strain relaxation in the island causes a strain concentration at the island edge. This leads to strain dependent kinetic barriers for adatoms to diffuse to the island surface. These kinetic barriers are increased as the island size increases which helps to a gradual reduction of the island growth rate [22]. In the case treated here, highest values of lattice distortion are found for samples grown at highest temperatures, which indeed corresponds to the highest island formation case.

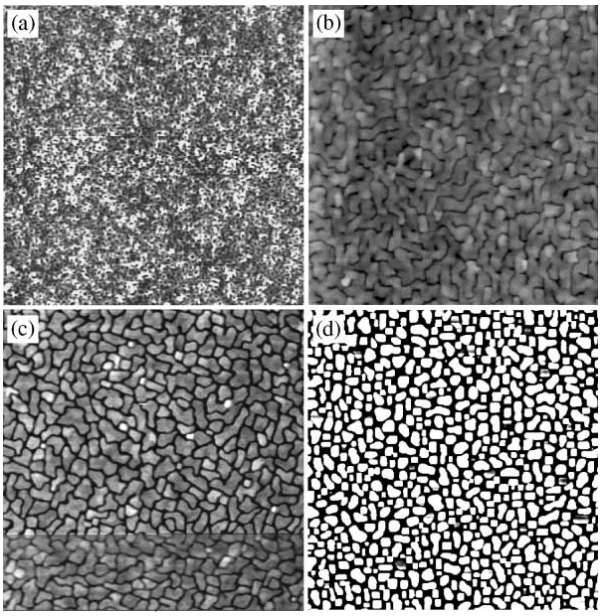


Fig. 3. AFM images for a series of Pt/Fe/MgO/GaAs(0 0 1) samples with Fe layers deposited at different temperatures: (a) 300°C, (b) 400°C, (c) 500°C and (d) 700°C. Lateral scanned dimensions: 5 μm × 5 μm. Grey scale: 20 nm height from black to white.

WD EX1084
Western Digital v IP Bridge
Page 227

## 4. Epitaxial Fe/MgO multilayered structures

Next step in the fabrication of a Fe/MgO multilayered structure was the epitaxy of MgO on Fe. In Fig. 4(a) we show RHEED patterns for a 20 Å MgO layer deposited by laser ablation at 400°C on a Fe thin film. The symmetry obtained is equivalent to one of the MgO buffer layer, the diffraction lines being sharper and more intense now, as compared with Fig. 1(a). This improvement in the structure can be easily understood taking into account the respective lattice mismatches between MgO and Fe or GaAs, respectively. The absolute lattice mismatch between MgO and GaAs amounts −25%, but turns out to be −0.6% considering a 4MgO/3GaAs registry. This gives rise to a pretty incoherent interface with one additional MgO in plane cell every three GaAs cells. On the other hand, the lattice mismatch between MgO and Fe is of 3.8% upon a 45° rotation of the MgO lattice with respect to the Fe (the equivalent well known behaviour observed for Fe/MgO(0 0 1)). This implies that the MgO/Fe interface has a much higher degree of crystalline coherency as compared with the MgO/GaAs interface, and therefore, the crystalline quality of MgO is higher when grown on Fe than when grown on GaAs under identical experimental conditions.

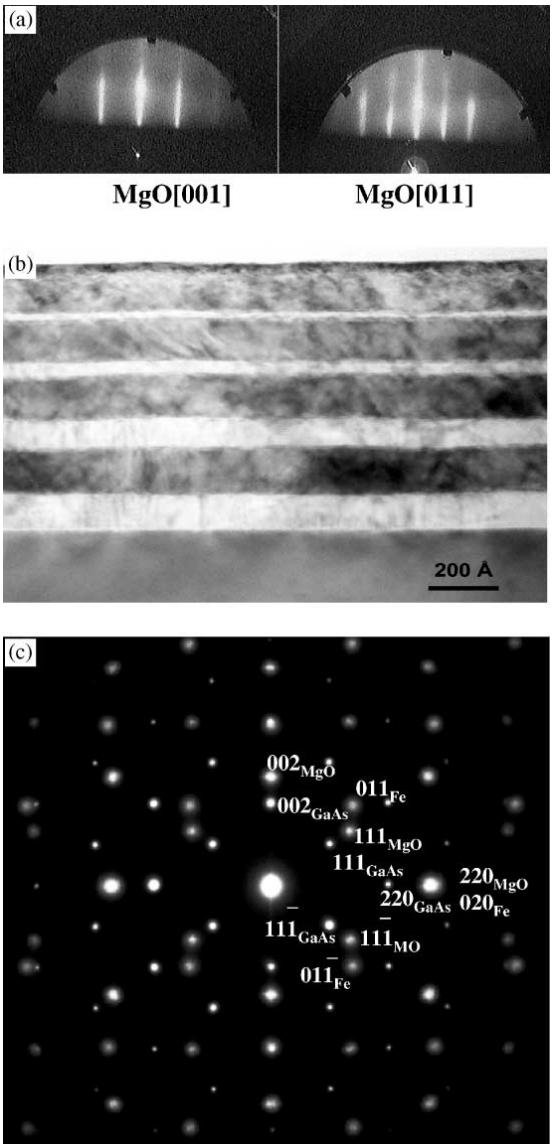


Fig. 4. (a) RHEED patterns along [1 0 0] and [1 1 0] azimuths for a MgO layer grown on Fe(0 0 1) at 400°C. (b) Cross-section TEM image of a Fe/MgO(0 0 1) multilayer with gradually decreasing MgO thickness. Fe layers (80 Å thick) were grown at RT and annealed at 400°C. MgO layers (80, 60, 40 and 20 Å thick) were grown at 400°C. (c) Selected area electron diffraction pattern along the [1 $\bar{1}$ 0] axis.

Taking advantage of both Fe/MgO and MgO/Fe epitaxies, we have designed a multilayered structure composed of several Fe/MgO bilayers, all of them with equivalent Fe layer thickness (80 Å) and gradually decreasing MgO thickness (from 80 down to 20 Å). This specific structure permits us to obtain information about the lowest MgO thickness compatible with continuous, pinhole free layer, which is mandatory for example to obtain operating magnetic tunnel junctions. In this case, Fe films were grown at RT and annealed at 400°C, while MgO layers were grown at 400°C. RHEED patterns for the different subsequent layers are equivalent to those shown in Fig. 1(c) and (d) for unnanealed and annealed Fe and Fig. 4(a) for MgO. In Fig. 4(b) a [1 1 0] cross-section TEM image from this test structure. Notice that on top of the GaAs substrate, the Fe layers appear in dark contrast while bright regions are the MgO layers. Continuous and good crystal quality MgO films with sharp interfaces are obtained all the way down to the thinnest oxide layer. No evidence of pinhole across the MgO barriers has been detected, not only from this

WD EX1084
Western Digital v IP Bridge
Page 228

image but also from the rest of the thin foil regions examined. Further confirmation of the crystallinity and high quality of the structure can be seen in Fig. 4(c), were we show a selected area electron diffraction pattern of a typical MgO[1 $\bar{1}$ 0]‖Fe[1 0 0]‖MgO[1 $\bar{1}$ 0]‖GaAs[1 $\bar{1}$ 0] sample with [0 0 1] as growth direction. Lattice parameters agree almost completely with bulk parameters, i.e. layers are relaxed.

To show the dramatic influence that Fe growth temperature can have in the continuity of a Fe/MgO multilayered structure, another test sample equivalent to the one shown in Fig. 4(b) was fabricated. In this case, growth temperature was kept equal to 400°C during the entire deposition process, temperature at which Fe morphology exhibits a strong dendritic character. RHEED patterns for this structure are as well indicative of fully Fe and MgO epitaxial growth. In Fig. 5, we show two XTEM images for this structure, where again dark and bright contrast regions correspond to Fe and MgO, respectively. Big single crystalline Fe islands are formed with very flat surfaces parallel to the substrate plane and in-plane sizes between 130 and 30 nm. Some other islands sides also correspond to crystallographic Fe planes, as indicated in Fig. 5(b). On the other hand, MgO layers are observed to cover the empty spaces left by the Fe islands, the effect being less clear as growth proceeds due to the intentional reduction in deposited amount of MgO. All the interfaces between MgO and GaAs as well as with most of the faces of the Fe islands are sharp and very flat, indicative of a low degree of intermixing. Finally, Pt capping layer is also clearly observable (Fig. 5(a)), with a high degree of conformality with respect to the underneath surface.

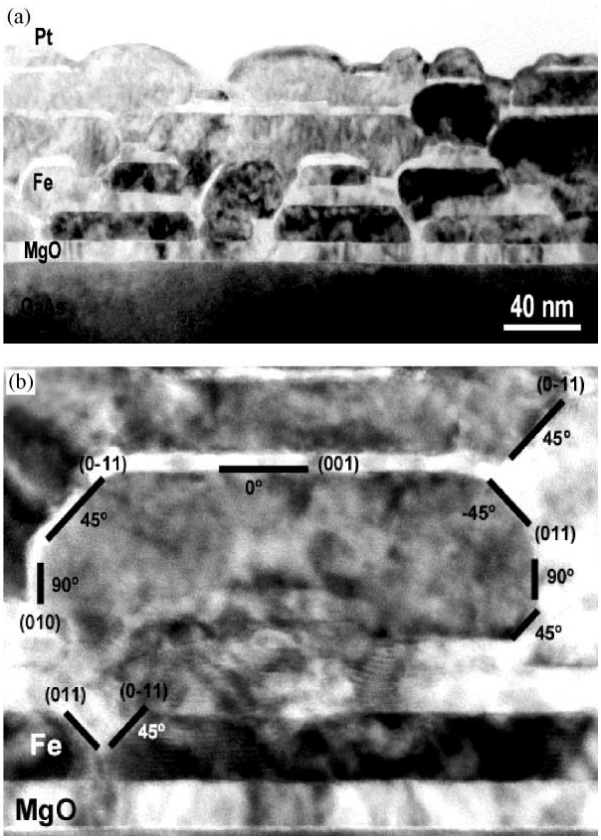


Fig. 5. (a) Cross-section [1 1 0] TEM image of a Fe/MgO(0 0 1) multilayer equivalent to that shown in Fig. 4 but grown at 400°C. (b) Selected area showing an indexed monocrystalline island with well defined facets along (0 1 0), (0 ±1 1) and (0 0 1) axis.

## 5. Conclusions

In this work, the possibility to obtain epitaxial metal/insulator multilayered heterostructures on GaAs(0 0 1) substrates has been demonstrated. We have first performed a study of different Fe thin films deposited of MgO buffered GaAs substrates. Analysing Fe films morphology, a gradual transition from 2D to 3D growth modes is found for temperatures in the range 300–400°C. We attribute the origin of this transition to stress and its relaxation as the driving force altering both surface and step edge diffusion barriers. As a second step, epitaxy of MgO thin films on the previously deposited Fe layers is also demonstrated, opening new directions for the fabrication of fully epitaxial metal/insulator heterostructures on semiconductor substrates. To confirm this assertion, two Fe/MgO multilayered epitaxial heterostructures have been fabricated following different thermal procedures. These structures can exhibit continuous and flat interfaces if appropriate growth conditions are selected.

WD EX1084
Western Digital v IP Bridge
Page 229

## Acknowledgements

Work performed under financial support of the Spanish Commission of Science and Technology. We thank M. Tello and R. García for the AFM measurements.

## References

[1] G.A. Prinz, Science 282 (1998) 1660.
[2] S.S.P. Parkin, K.P. Roche, M.G. Samant, P.M. Rice, R.B. Beyers, R.E. Scheuerlein, E.J. O'Sullivan, S.L. Brown, J. Bucchigano, D.W. Abraham, M.Rooks Yu Lu, P.L. Trouilloud, R.A. Wanner, W.J. Gallagher, J. Appl. Phys. 85 (1999) 5828.
[3] J.S. Moodera, L.R. Kinder, T.M. Wong, R. Meservey, Phys. Rev. Lett. 74 (1995) 3273.
[4] G.A. Prinz, J.J. Krebs, Appl. Phys. Lett. 39 (1981) 397.
[5] T. Kado, J. Crystal Growth 144 (1994) 329.
[6] T. Kado, Appl. Phys. Lett. 69 (1996) 1393.
[7] D.K. Fork, K. Nashimoto, T.H. Geballe, Appl. Phys. Lett. 60 (1992) 1621.
[8] L.S. Hung, L.R. Zheng, T.N. Blanton, Appl. Phys. Lett. 60 (1992) 3129.
[9] E.J. Tarsa, M.D. Graef, D.R. Clarke, A.C. Gossard, J.S. Speck, J. Appl. Phys. 73 (7) (1993) 3276.
[10] P.A. Stampe, R.J. Kennedy, Thin Solid Films 326 (1998) 63.
[11] T. Urano, T. Kanaji, J. Phys. Soc. Japan 57 (1998) 3403.
[12] M. Dynna, J.L. Vassent, A. Marty, B. Gilles, J. Appl. Phys. 80 (1996) 2650.
[13] J.L. Vassent, M. Dynna, A. Marty, B. Gilles, G. Patrat, J. Appl. Phys. 80 (1996) 5727.
[14] D.J. Keavney, E.E. Fullerton, S.D. Bader, J. Appl. Phys. 81 (1997) 795.
[15] W. Wulfhekel, M. Klaua, D. Ullmann, F. Zavaliche, J. Kirschner, R. Urba, T. Monchesky, B. Heinrich, Appl. Phys. Lett. 78 (2001) 509.
[16] W.H. Butler, X.G. Zhang, T.C. Schultess, J.M. MacLaren, Phys. Rev. B 63 (2001) 54416.
[17] E.E. Fullerton, D.M. Kelly, J. Gimpel, Y.K. Schuller, Phys. Rev. Lett. 68 (1992) 859.
[18] C. Martínez Boubeta, J.L. Menéndez, J.L. Costa-Krämer, J.M. García, J.V. Anguita, B. Bescós, A. Cebollada, F. Briones, A.V. Chernykh, I.V. Malikov, G.M. Mikhailov, Surf. Sci., in press.
[19] K. Nashimoto, D.K. Fork, T.H. Geballe, Appl. Phys. Lett. 60 (1992) 1199.
[20] J.L. Menéndez, P. Caro, A. Cebollada, J. Crystal Growth 192 (1998) 164.
[21] H. Röder, K. Bromann, H. Brune, K. Kern, Surf. Sci. 376 (1997) 13.
[22] Y. Chen, J. Washburn, Phys. Rev. Lett. 77 (1996) 4046.

**WD EX1084**
**Western Digital v IP Bridge**
**Page 230**